A New Method for Segmenting Individual Trees from the Lidar Point Cloud

Wenkai Li, Qinghua Guo, Marek K. Jakubowski, and Maggi Kelly

Abstract

Light Detection and Ranging (lidar) has been widely applied to characterize the 3-dimensional (3D) structure of forests as it can generate 3D point data with high spatial resolution and accuracy. Individual tree segmentations, usually derived from the canopy height model, are used to derive individual tree structural attributes such as tree height, crown diameter, canopy-based height, and others. In this study, we develop a new algorithm to segment individual trees from the small footprint discrete return airborne lidar point cloud. We experimentally applied the new algorithm to segment trees in a mixed conifer forest in the Sierra Nevada Mountains in California. The results were evaluated in terms of recall, precision, and F-score, and show that the algorithm detected 86 percent of the trees ("recall"), 94 percent of the segmented trees were correct ("precision"), and the overall F-score is 0.9. Our results indicate that the proposed algorithm has good potential in segmenting individual trees in mixed conifer stands of similar structure using small footprint, discrete return lidar data.

Introduction

Light Detection and Ranging (lidar) is an active remote sensing technology that measures properties of reflected light to determine range to a distant object (Lefsky *et al.*, 2002). The range to an object is calculated by measuring the time delay between transmission of a laser pulse and detection of the reflected signal (Wehr and Lohr, 1999). Due to its ability to generate 3-dimensional (3D) data with high spatial resolution and accuracy, lidar technology is being increasingly used in ecology (Lefsky *et al.*, 2002; Gaveau and Hill, 2003; Hopkinson *et al.*, 2004a; Hopkinson *et al.*, 2004b), geomorphology (Glenn *et al.*, 2006), seismology (Lee *et al.*, 2009), and remote sensing (Brandtberg *et al.*, 2003).

Individual tree segmentations have significant implications in forestry (Chen *et al.*, 2006; Koch *et al.*, 2006; Chen *et al.*, 2007). Once accurately segmented, tree structural attributes such as tree height, crown diameter, canopy based height, basal area, diameter at breast height (DBH), wood volume, biomass, and species type can be derived (Chen *et al.*, 2007; Korpela *et al.*, 2007; Yu *et al.*, 2011). Traditional methods for characterizing the 3D structure of forest stands, and capturing individual tree characteristics include field inventory and aerial photography interpretation, yet both methods have limitations that can be overcame using lidar (Lang *et al.*, 2006). Field inventories can be labor-intensive,

time-consuming, and limited by spatial accessibility (Lee *et al.*, 2010); and optical aerial photography does not directly provide 3D forest structure information (Chen *et al.*, 2006). Recently, lidar has been widely and successfully applied in forest research (Naesset and Bjerknes, 2001; St-onge and Achaichia, 2001; Popescu *et al.*, 2002; Lim *et al.*, 2003; Popescu *et al.*, 2003; Patenaude *et al.*, 2004; Popescu and Wynne, 2004; Riaño *et al.*, 2004; Suárez *et al.*, 2005; Popescu, 2007; Chasmer *et al.*, 2008; Stephens *et al.*, 2008; Huang *et al.*, 2009), and it shows promise to map individual trees in complex and heterogeneous forests (Brandtberg *et al.*, 2003; Popescu and Wynne, 2004; Chen *et al.*, 2006; Koch *et al.*, 2006; Chen *et al.*, 2007).

There are numerous methods proposed to delineate individual trees using airborne lidar data. For example, Popescu and Wynne (2004) used a local maximum filtering technique to locate and measure individual trees. Tiede *et al.* (2005) used a similar local maximum algorithm to identify tree tops and then developed a region growing algorithm to delineate tree crowns. Chen *et al.* (2006) proposed a marker-controlled watershed segmentation to isolate individual trees; the tree tops identified by local maxima were used as markers to improve the accuracy. Koch *et al.* (2006) delineated tree crowns with a combination of a pouring algorithm, knowledge-based assumptions on the shape of trees, and a final detection of the crown-edges. Korpela *et al.* (2007) used a multi-scale template matching approach for tree detection and measurement. They used elliptical and other shaped templates to represent tree models. The spatial wavelet analysis has also been proposed to automatically determine the location, height, and crown diameter of individual trees from lidar data (Falkowski *et al.*, 2006).

What these segmentation algorithms share is that they segment individual trees using the lidar-derived canopy height model (CHM), which is a raster image interpolated from lidar points depicting the top of the vegetation canopy. This is not ideal, as the CHM can have inherent errors and uncertainties from a number of sources. For example, spatial error can be introduced during the interpolation process from the point cloud to the gridded height model (Guo *et al.*, 2010), which can decrease the accuracy of tree segmentations and relevant measurements. Therefore, new methods to segment individual trees directly from the lidar point cloud need to be developed and enhanced. Morsdorf *et al.* (2003) used the *k*-mean clustering algorithm to segment individual trees from the point cloud, but their accuracy depended on seed points extracted from the local maxima of a rasterized

---

Wenkai Li and Qinghua Guo are with the Sierra Nevada Research Institute, School of Engineering, University of California, Merced, CA 95343 (qguo@ucmerced.edu).

Marek K. Jakubowski and Maggi Kelly are with the Department of Environmental Sciences, Policy & Management, University of California, Berkeley, CA 94720.

digital surface model, and thus this method did not directly rely on the lidar point cloud. Lee *et al.* (2010) developed an adaptive clustering approach to segment individual trees in managed pine forests from the raw lidar 3D point data; the method is similar to the concept of watershed segmentation, but it requires sufficient training data for supervised learning, and its performance in complex forests has not been tested.

In this study, we develop a new algorithm to segment individual trees directly from the lidar point cloud. To investigate the algorithm's effectiveness in segmenting individual trees, we apply our algorithm to isolate individual trees in a mixed conifer forest using small footprint, discrete return, high-density airborne lidar data. Detailed descriptions about the algorithm, evaluation of its performance, and discussion of the implications of the method are provided in the following sections.

Methods

Study Site and Datasets
Our study area (118 km²) is located in the Sierra National Forest, on the western slope of the central Sierra Nevada Mountains of California (Figure 1) (37°26′N 119°35′W; 1,300 to 1,800 m above sea level). The area is characterized by Sierra mixed conifer forest dominated by white fir (*Abies concolor*), ponderosa pine (*Pinus ponderosa*), incense cedar (*Calocedrus decurrens*), sugar pine (*Pinus lambertiana*), and giant sequoia (*Sequoiadendron giganteum*) with black oak (*Quercus kelloggii*) and canyon live oak (*Quercus chrysolepis*) as the major hardwoods within the stands.

Lidar data were acquired between 13 September and 15 September 2007. We contracted with the National Center for Airborne Laser Mapping (NCALM) who used an Optech GEMINI Airborne Laser Terrain Mapper (ALTM) mounted in a twin-engine Cessna Skymaster. The Optech ALTM sensor recorded up to four echoes per pulse. The sensor operated at 100 kHz, with a scanning frequency of 40 Hz and the total scan angle of ± 24°. One hundred and three individual

Figure 1. Study area and testing plots.

flight lines were flown to cover the study area. The swath width of a single pass averaged 509.56 m, with planned line spacing at 168.15 m. Planned overlap was 341.4 m: all of the ground area was covered with shots from three different swaths, with four swaths in many cases. Average flight speed was 61.7 m/s at a mean altitude of 700 m above ground level. The target point density (>6 points/m²) was met by using 67 percent overlap of adjacent flight lines and line spacing of 168.15 m. The horizontal accuracy was 1:11,000 of the flying altitude and the vertical accuracy was 5 to 10 cm.

In this study, we selected 20 circular plots (12.62 m radius) that provided a range of tree densities over the study site for accuracy assessment (Figure 1). All plot centers were greater than 12.62 m from any landing or road surface. We used the Trimble GeoXH GPS and TruPulse™ 360 to georeference the locations of plot centers and individual trees inside the plots. The georeferenced trees were manually verified and refined by comparing to the lidar point cloud with the 3D visualization in Esri ArcScene® software. Trees that were not georeferenced in the field survey were manually marked and delineated from the point cloud. We obtained 380 reference trees in total, and the number of trees within each plot averaged 19 and varied from 9 to 35.
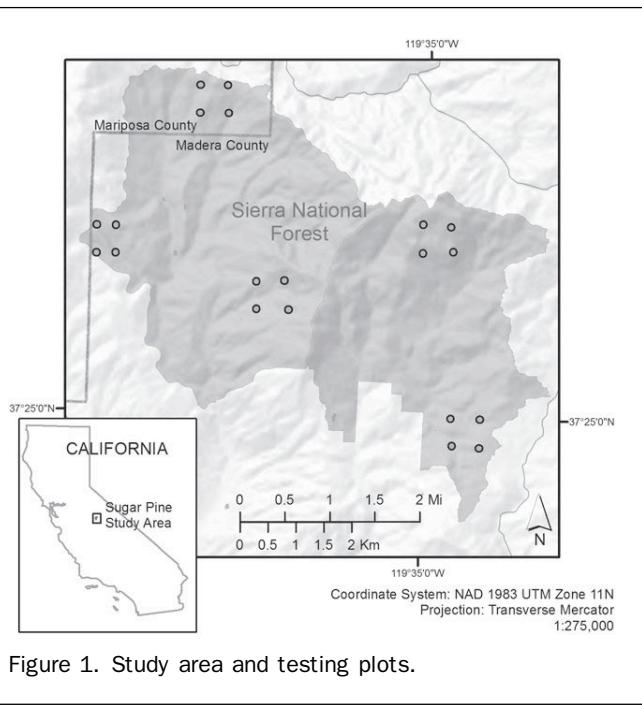
Individual Tree Segmentations
Preprocessing
TerraSolid's TerraScan (**http://terrasolid.fi**) software was used to classify the raw lidar point data into ground and above-ground points. Ordinary kriging was used to interpolate the ground points and generate the digital elevation model (DEM) at 1 m resolution (Guo *et al.*, 2010). The above-ground (vegetation) points were used for tree segmentation. We normalized the vegetation point cloud values by subtracting the ground points (DEM) from the lidar point cloud (Lee *et al.*, 2010). After normalization, the elevation value of a point indicates the height from the ground to the point (Figure 2). If the point is the tree top, its height value can be considered as the tree height.

The Algorithm
Our method works by segmenting trees individually in sequence from the point cloud by taking advantage of the relative spacing between trees (Figure 3). In general, there is horizontal spacing between trees and the spacing at the top of a tree is larger than the spacing at the bottom as show in Figure 3a. Although trees may overlap in dense stands, there is still spacing between them at the higher level, as show in Figure 3b. Hence, starting from a tree top, we can identity and "grow" a target tree by including nearby points and exclude points of other trees based on their relative spacing. It becomes increasingly difficult to classify points at the lower level because the spacing between trees decreases, particularly for overlapping trees. To overcome this challenge, the points are classified sequentially, from the highest to the lowest. Points with spacing larger than a specified threshold are excluded from the target tree; points with spacing smaller than the threshold are classified based on a minimum spacing rule. For example, in Figure 4, point A is the highest and hence considered as the top of tree #1 (target). Starting from the seed point A, we classify other lower points sequentially. First, point B is classified as tree #2 because the spacing d_{AB} is bigger than a specified threshold (e.g., 2 m). We then consider point C whose spacing d_{AC} is smaller than the threshold. By comparing to points A and B, point C is classified as tree #1 because d_{AC} is smaller than d_{BC}. Sequentially, point D is classified as tree #2 by comparing
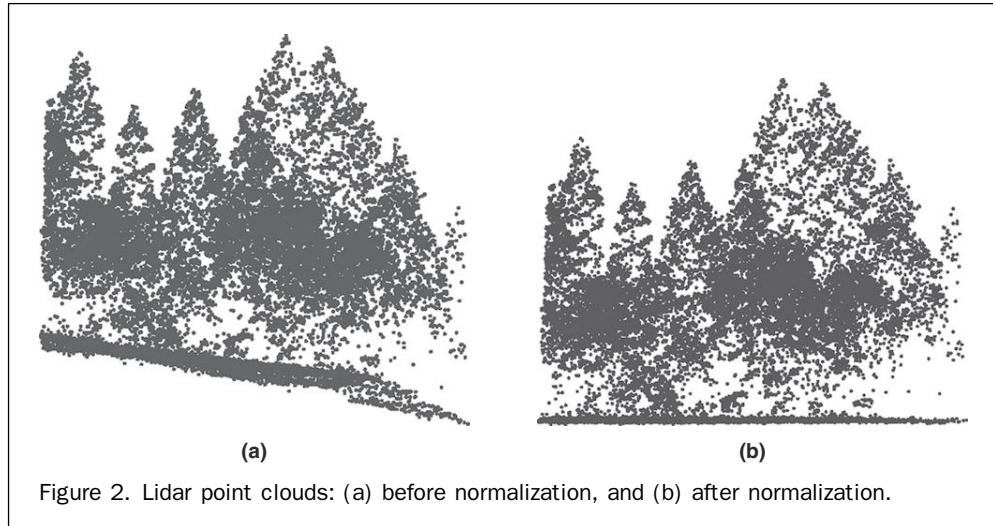
Figure 2. Lidar point clouds: (a) before normalization, and (b) after normalization.
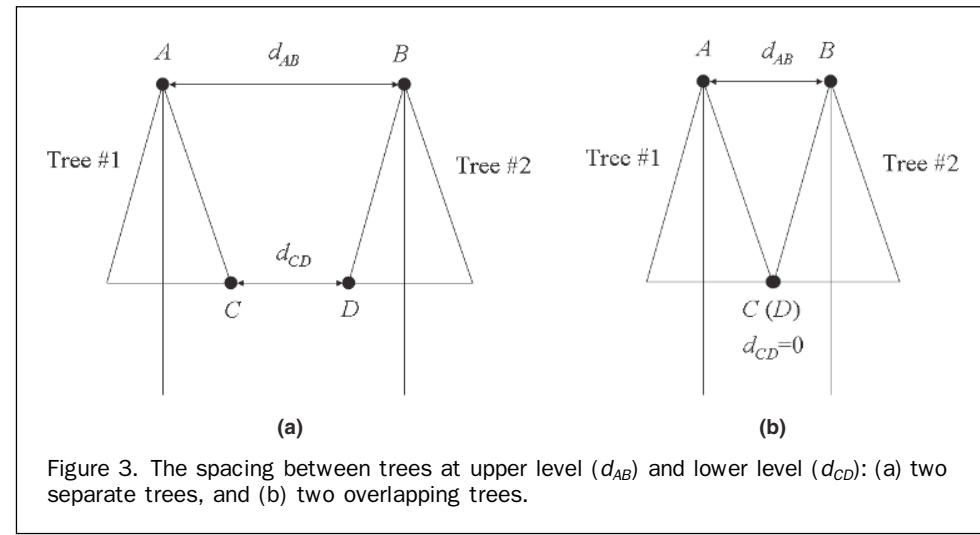

Figure 3. The spacing between trees at upper level (d_{AB}) and lower level (d_{CD}): (a) two separate trees, and (b) two overlapping trees.
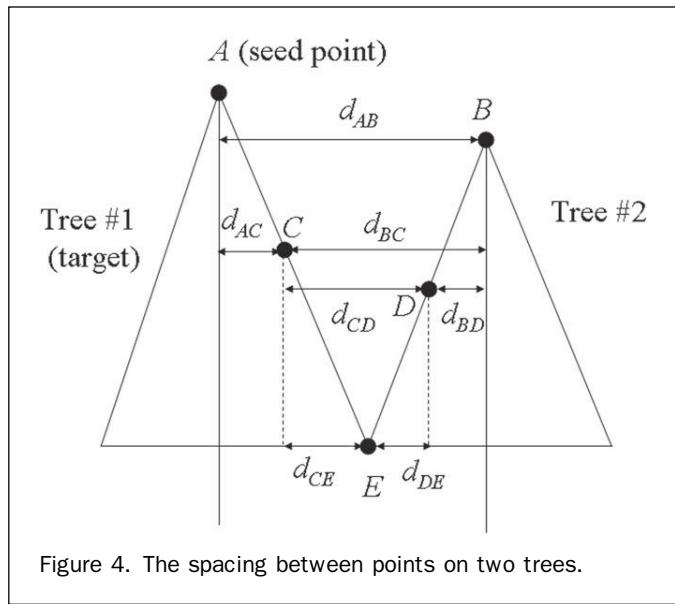

Figure 4. The spacing between points on two trees.

to points B and C, and point E is classified as tree #2 by comparing to points C and D.

By defining an appropriate spacing threshold, most of the points can be correctly assigned to their corresponding tree clusters. The threshold should be approximately equal to the crown radius. If the threshold is too small, trees with elongated branches may be over-segmented; if the threshold is too large, nearby trees may be missed. Consider Figure 5 as an example. If the threshold d_{AB} is used, point B is correctly assigned to tree #1. Next, point C will be compared to point B and falsely assigned to tree #1 because the spacing d_{BC} is smaller than the threshold d_{AB}, resulting in tree #2 not being segmented (under-segmentation). In contrast, if the threshold d_{BC} is used, point B is falsely excluded from tree #1 (over-segmentation). Meanwhile, point C is correctly excluded from tree #1 and hence tree #2 can be detected and segmented later. To solve the problem, an adaptive threshold can be used, assuming that taller trees have larger crown diameters (Popescu and Wynne, 2004; Chen *et al.*, 2006).

Additionally, more classification rules can be added to improve the accuracy of the segmentation. In Figure 6, point A is identified as the top of tree #1 (target), and the next
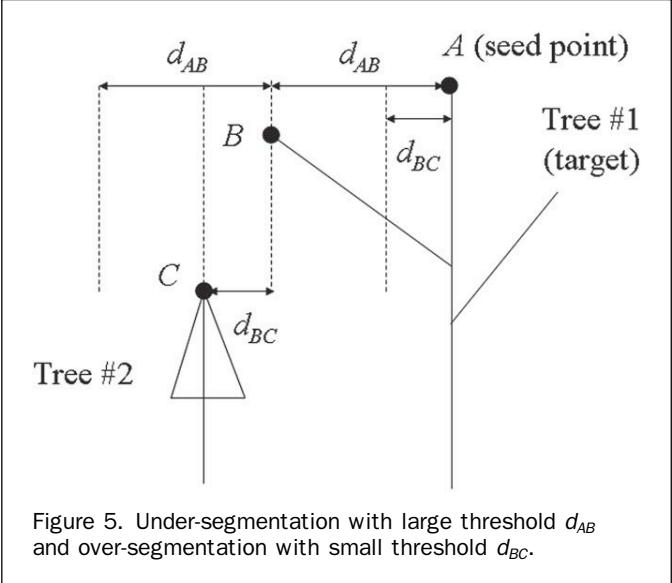
Figure 5. Under-segmentation with large threshold d_{AB} and over-segmentation with small threshold d_{BC}.

point to be classified is B. The spacing d_{AB} is larger than a defined threshold, and B can be the top of an elongated branch of tree #1 (Figure 6a), or the top of tree #2 (Figure 6b). If the points approximate to B are projected into a 2D Euclidean space, the convex hull of these points is more elongated for the branch (Figure 6a), and more compact for a separate tree (Figure 6b). The shape of the convex hull can be indicated by a shape index (SI):

$$SI = \frac{P}{4 \times \sqrt{A}} \qquad (1)$$

where P is the perimeter, and A is the area of the convex hull. Alternatively, we can also use a relative shape index that corrects for the size problem on the simple perimeter-area ratio (Guo *et al.*, 2007). A higher value of the shape index indicates a more elongated shape. Hence, a threshold
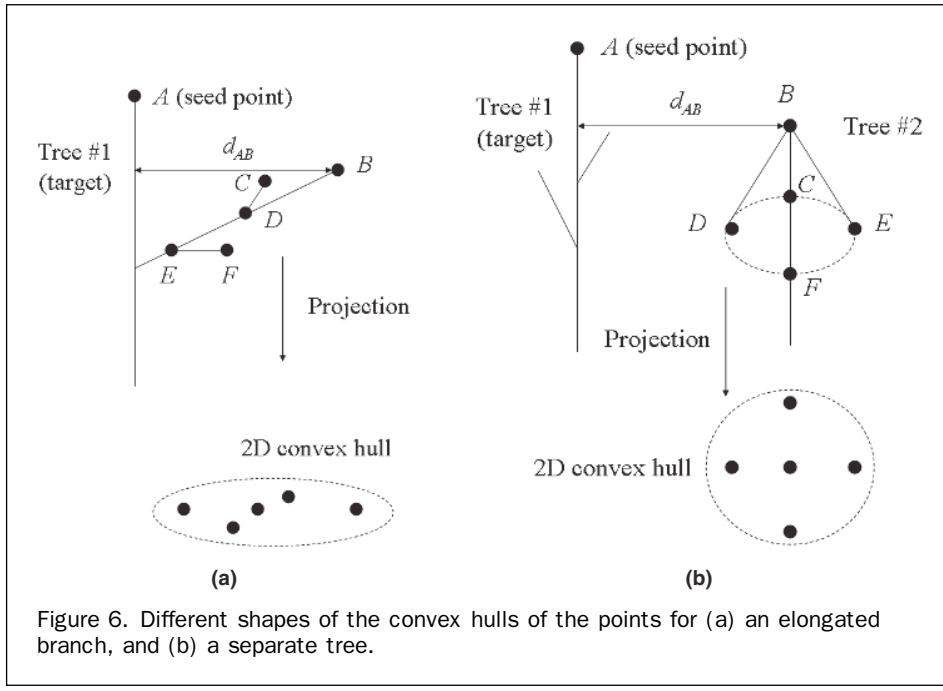
of the shape index can be used to differentiate between a branch and a tree.

If a branch is detected, there are two possibilities: it belongs either to the target tree or to a nearby tree. We can differentiate these two cases according to the distribution of the points. In Figure 7, point C is the top of an elongated branch, and points D, E, and F are approximate to C within a search radius. When projected into 2D Euclidean space, most of the points fall into the left sector if the branch belongs to tree #1 (Figure 7a). By contrast, most of the points fall into the right sector if the branch belongs to tree #2 (Figure 7b).

In summary, the trees are segmented based on a spacing threshold (either fixed or adaptive thresholds), a minimum spacing rule, and a horizontal profile of the tree shape. Under-segmentations can be reduced by using a relatively small threshold, and over-segmentations can be reduced based on the shape and distribution of the points. In addition, this algorithm is flexible and the classification rules are object-oriented, which can be modified or extended depending on the characteristics of the trees to be segmented.

Implementation

The proposed segmentation algorithm isolates trees individually and sequentially from the point cloud, from the tallest tree to the shortest. Let U_i denote a set of points to be segmented, P_i denote a set of points that belong to tree i (target), and N_i denote a set of points that do not belong to tree i. For iteration i, we classify each point in U_i as P_i or N_i. During each iteration, only one tree (target) is segmented, and the points corresponding to this target tree are removed from the point cloud. Therefore, for iteration $i + 1$, $U_{i+1} = U_i - P_i$. We start from the highest tree with $i = 1$ where U_1 is the original point cloud, and stop when U_i is empty. Figure 8 shows the flowchart of the algorithm.

During each iteration, we adopt a top-to-bottom approach to classify the points, i.e., we classify the points in U_i one by one, starting from the highest point to the lowest one. First, we find the highest point t_0 (global maximum) in U_i, which is assumed to be the top of the tallest tree i in U_i.

Figure 6. Different shapes of the convex hulls of the points for (a) an elongated branch, and (b) a separate tree.
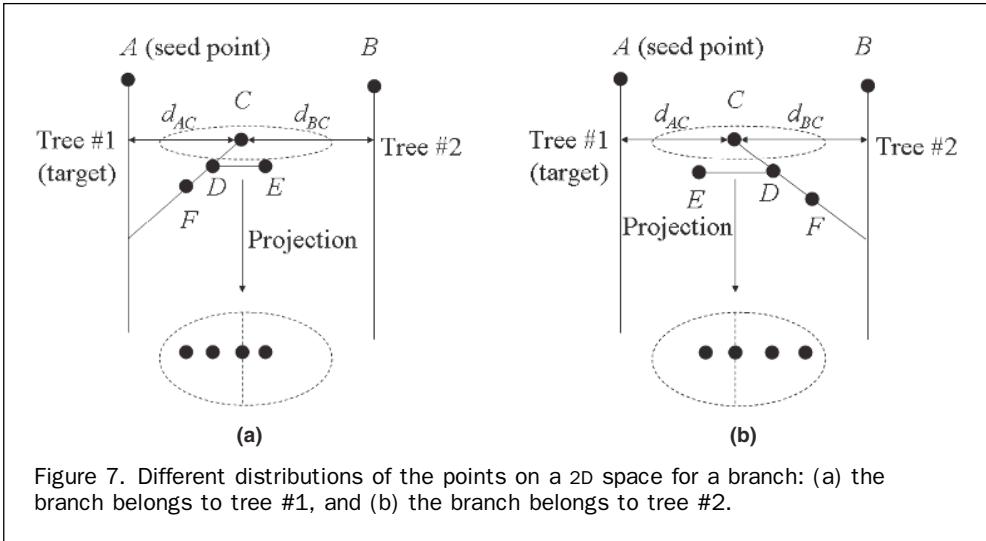
Figure 7. Different distributions of the points on a 2D space for a branch: (a) the branch belongs to tree #1, and (b) the branch belongs to tree #2.
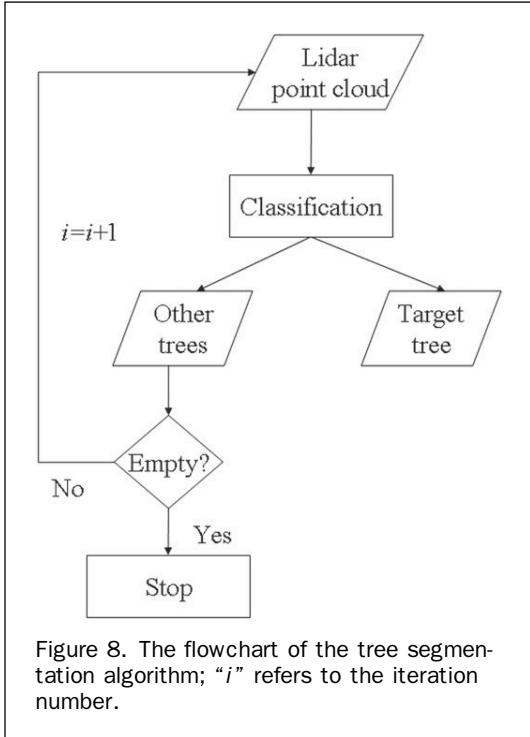

Figure 8. The flowchart of the tree segmentation algorithm; "i" refers to the iteration number.

Obviously, $t_0 \in P_i$. At this point, N_i is empty. We then insert a dummy point n_0 that is far away (e.g., 100 m) from t_0 into N_i. The basic idea is to use t_0 and n_0 as the initial seeds, and grow the clusters of P_i and N_i by finding their approximate points based on the rules mentioned previously. The growing directions are from top to bottom, and from center to boundary. Let u denote a point to be classified, and Z_u denote its height. Let $dmin_1$ denote the minimum distance from u to any point in P_i, and $dmin_2$ denote the minimum distance from u to any point in N_i. Note that here "distance" refers to the 2D Euclidean distance. Within a search radius R, the highest point is called local maximum, and any other lower point is called non-maximum. Note that the segmentation result is not sensitive to the search radius, and $R = 2$ m should be sufficient in most cases according to our test. We classify u using the following rules.

1. If the point u is the local maximum, it can be the top of a branch or the top of another tree. In this study we use the spacing threshold and minimum spacing rules to classify u:

   if $dmin_1 > d_t$, $u \in N_i$;
   if $dmin_1 <= d_t$ and $dmin_1 <= dmin_2$, $u \in P_i$;
   if $dmin_1 <= d_t$ and $dmin_1 > dmin_2$, $u \in N_i$

   where d_t is an adaptive threshold:
   $d_t = 2$ m if $Z_u > 15$ m;
   $d_t = 1.5$ m if $Z_u <= 15$ m.

   These parameters were determined by trial-and-error. It is reasonable to assume that the crown diameter of a tree is greater than 1 m, and that the tree spacing at the upper lever is greater than 1 m. Therefore, the parameters in this study can be used as the default, but users should tune them based on the tree spacing in the study area.
2. If u is a non-maximum point, it is simply classified based on the minimum spacing rule:

   if $dmin_1 <= dmin_2$, $u \in P_i$;
   if $dmin_1 > dmin_2$, $u \in N_i$.

The algorithm iterates until all points are classified into corresponding sets.

Accuracy Assessment
After running the tree segmentation algorithm, we compared the segmented trees with the reference trees in 20 testing plots. There are three types of tree segments and levels of accuracy produced (Plate 1). If a tree is correctly segmented, it is called true positive (*TP*); if a tree is not segmented but assigned to a nearby tree, it is called false negative (*FN*) or omission error; if a tree does not exist but is segmented from the point cloud, it is called false positive (*FP*) or commission error. *TP*, *FN*, and *FP* indicate perfect segmentation, under-segmentation, and over-segmentation, respectively. To evaluate the accuracy, we calculated recall (*r*), precision (*p*), and *F*-score using the following equations (Goutte and Gaussier, 2005; Sokolova *et al.*, 2006):

$$r = \frac{TP}{TP + FN} \tag{2}$$

$$p = \frac{TP}{TP + FP} \tag{3}$$

$$F = 2 \times \frac{r \times p}{r + p} \tag{4}$$

Plate 1. Three types of tree segments: (a) correctly detected tree (true positive, TP), (b) undetected tree (false negative, FN), and (c) falsely detected tree (false positive, FP). The posts indicate ground truth trees; the color of points indicates individual tree segments.

Recall indicates the tree detection rate, precision indicates the correctness of the detected trees, and *F*-score is the overall accuracy taking both commission and omission errors into consideration. The values of *r*, *p*, and *F* vary from 0 to 1. In order to obtain a higher *F*-score, both *r* and *p* should be high. For example, if all of the trees are correctly segmented (perfect segmentations), the values of *r* and *p* are one, resulting in *F* being equal to one.

Results

Plate 2a and 2b shows the comparison between the original and segmented point clouds for a 50 × 50 m area. It is apparent visually that most of the trees are correctly segmented. The tree segmentation results in other areas in our study are similar and hence are not shown here. Plate 2c and 2d shows the segmentation results for two typical plots. In the dense plot (Plate 2c), the tree spacing is small and some of the trees are missed and not segmented; in the sparse plot (Plate 2d), the tree spacing is large and most of the trees can be detected and segmented correctly.

The accuracy assessments for trees in the 20 test plots are shown in Table 1. The value of *r* varies from 0.71 to 1, with the overall value of 0.86; the value of *p* varies from 0.8 to 1, with the overall value of 0.94. In dense plots, trees are under-segmented and the value of *r* is relatively low. For example, 8 of the 31 trees in plot #10, and 10 of the 35 trees in plot #15 are not detected by the algorithm.

The corresponding values of *r* are only 0.74 and 0.71, respectively. However, the values of *p* in these two plots are 1, without errors of commission (falsely segmented trees). In contrast, the value of *r* in sparse plot is relatively high, but the value of *p* may be lower. For example, in plot #8, all of the 16 trees are correctly segmented, but there are 4 falsely detected trees. Consequently, the value of *r* is 1, but the value of *p* is only 0.8. The *F*-score, which considers both of these factors, varies from 0.83 to 0.95, with the overall value from all the plots of 0.90.

The relationship between the number of reference trees and the number of segmented trees per plot is shown in Figure 9. The correlation is relatively strong, with the correlation coefficient *r* = 0.91. In general, the number of trees is under-estimated with our method. There are 380 trees in total in our test plots, but only 347 trees are segmented. The algorithm missed 53 trees, and falsely detected 20 trees, with under-segmentation outweighing over-segmentation.

Discussion

Since the late 1990s, lidar has shown promise in forest science, for characterizing the structure of forests at landscape-scale, stand-scale, and plot-scales (Dubayah and Drake, 2000; Naesset and Bjerknes, 2001; Lim *et al.*, 2003; Riaño *et al.*, 2003; Popescu and Wynne, 2004). These efforts in forest quantification are currently driving improvements in fire
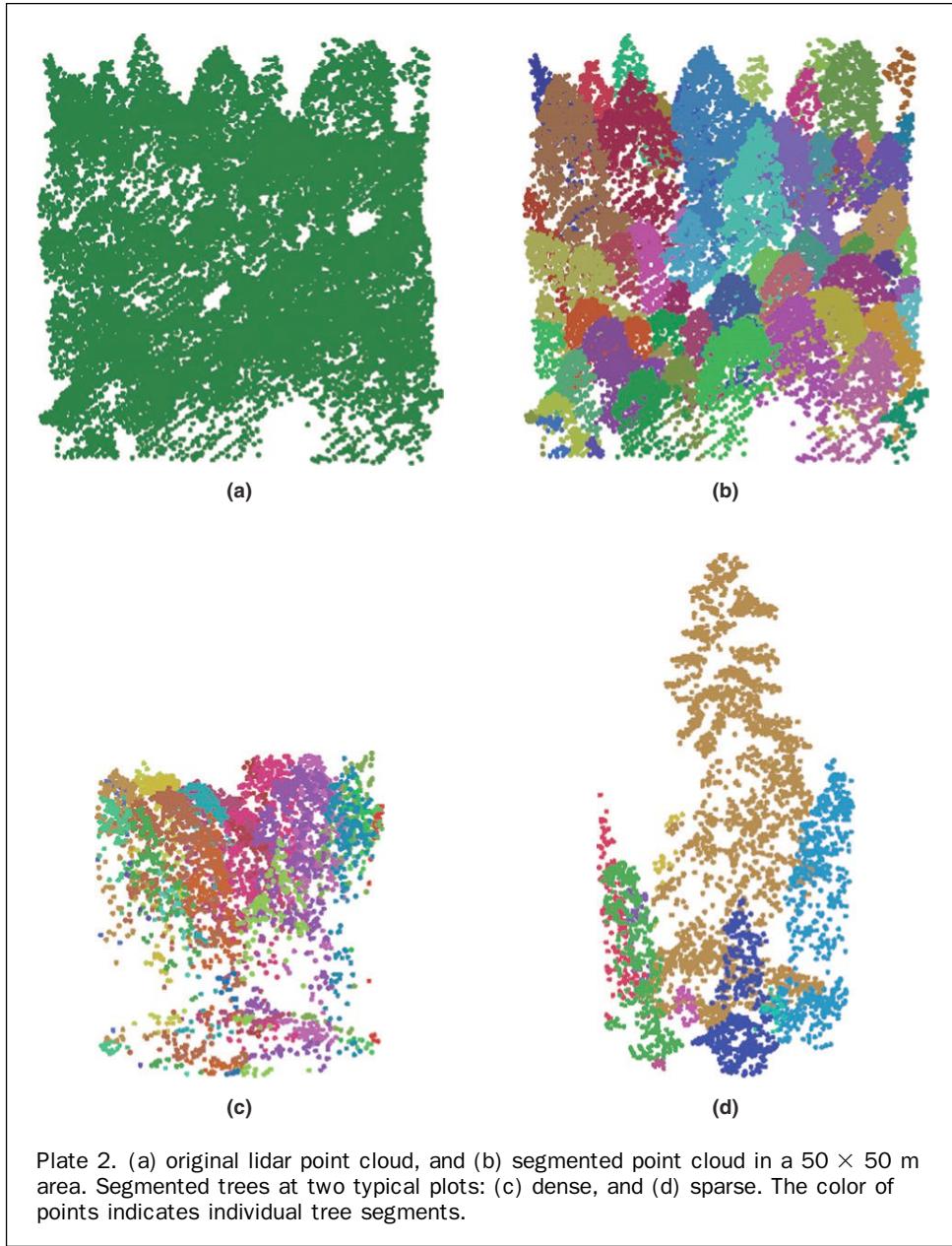
Plate 2. (a) original lidar point cloud, and (b) segmented point cloud in a 50 × 50 m area. Segmented trees at two typical plots: (c) dense, and (d) sparse. The color of points indicates individual tree segments.

modeling (Mutlu *et al.*, 2008; Wing *et al.*, 2010), and forest management (Wynne, 2006; Wulder *et al.*, 2008). Yet, further refinements in scale are still required for precise forest modeling. The successful identification and characterization of individual trees is critical in forest science, particularly for individual tree growth modeling (Falkowski *et al.*, 2010; Vepakomma *et al.*, 2011), linking with biometereological models (Chen *et al.*, 2008) and more precise measures of biomass in forests (Popescu *et al.*, 2003).

However, the accuracy of individual tree detection and delineation using lidar data is relatively low in complex and heterogeneous forests (Persson *et al.*, 2002). In some studies, only 40 to 80 percent of the trees are detected using lidar data (Heurich *et al.*, 2004; Tiede *et al.*, 2005; Chen *et al.*, 2006; Korpela *et al.*, 2007; Alexander, 2009). For example, Persson *et al.* (2002) found 71 percent of trees in the forest mainly consisting of spruce and pine; Kwak *et al.* (2007) reported accuracies from 60 to 80 percent in coniferous and deciduous forests; Yu *et al.* (2011) detected 69 percent trees

in a boreal forest area. Our algorithm, possibly in part because it makes use of non-transformed, raw point cloud, increases the accuracy of detected individual trees. Overall, about 86 percent of the trees in our study area were detected by the algorithm, and 94 percent of the segmented trees were correct. Our new algorithm shows good potential to delineate individual trees in mixed and complex coniferous forests. However, its effectiveness in other forest types like deciduous forests needs to be evaluated.

Our algorithm makes use of the 3D structure inherent in the lidar point cloud. It makes use of the shape of trees in a forest by taking advantage of the relative difference in spacing between tree tops and tree bases, and it incorporates a novel quantification of tree shape, as defined by the horizontal profile of a tree. Misclassifications may happen where the canopy is unequally sampled by the laser pulses, but this problem can be reduced by increasing the lidar point density. In our study the average lidar point density is larger than 6 points/m^2, and can reach up to 20 points/m^2 in

Plot ID	Number of trees	Density (trees/m²)	Number of segmented trees	TP	FP	FN	r	p	F
1	14	0.03	14	13	1	1	0.93	0.93	0.93
2	9	0.02	11	9	2	0	1.00	0.82	0.90
3	21	0.04	20	19	1	2	0.90	0.95	0.93
4	15	0.03	13	13	0	2	0.87	1.00	0.93
5	22	0.04	21	20	1	2	0.91	0.95	0.93
6	24	0.05	21	21	0	3	0.88	1.00	0.93
7	17	0.03	16	15	1	2	0.88	0.94	0.91
8	16	0.03	20	16	4	0	1.00	0.80	0.89
9	12	0.02	13	11	2	1	0.92	0.85	0.88
10	31	0.06	23	23	0	8	0.74	1.00	0.85
11	21	0.04	19	19	0	2	0.90	1.00	0.95
12	13	0.03	13	12	1	1	0.92	0.92	0.92
13	16	0.03	14	13	1	3	0.81	0.93	0.87
14	21	0.04	18	17	1	4	0.81	0.94	0.87
15	35	0.07	25	25	0	10	0.71	1.00	0.83
16	23	0.05	19	19	0	4	0.83	1.00	0.90
17	16	0.03	15	14	1	2	0.88	0.93	0.90
18	17	0.03	16	15	1	2	0.88	0.94	0.91
19	20	0.04	17	17	0	3	0.85	1.00	0.92
20	17	0.03	19	16	3	1	0.94	0.84	0.89
Overall	380	0.04	347	327	20	53	0.86	0.94	0.90

vegetated areas, which is sufficient to capture the 3D structure of individual trees.

Similar to other tree segmentation methods, tree top detection is the most important step in segmentation as it significantly affects the resulting accuracy. In the past, local maximum filtering techniques have been used to locate the tops of trees, but the size of search window is difficult to determine (Popescu and Wynne, 2004; Chen *et al.*, 2006), especially in dense and variable forest canopies. Our algorithm avoids this common problem by finding the global maximum, segmenting this target tree using classification rules, and then removing the resulting tree from the point cloud. Subsequently, the highest point in the remaining point cloud can be used as the top of the second highest
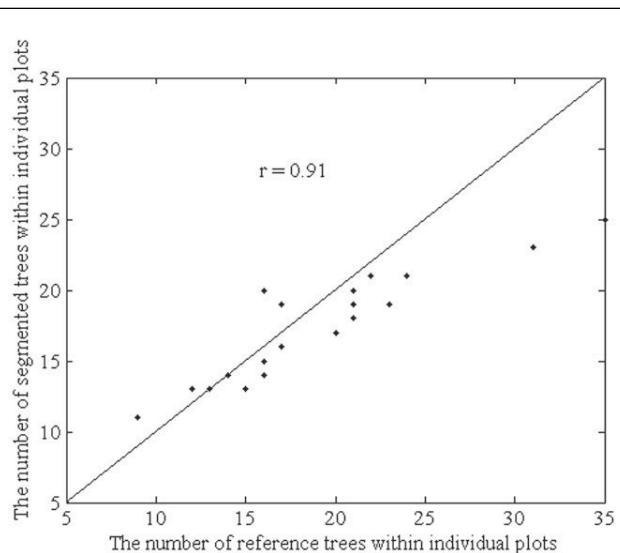

Figure 9. The relationship between the number of reference trees and the number of segmented trees within individual plots; "r" refers to the correlation coefficient.

tree, and so on. Trees are thus segmented individually, and sequentially, from the highest to the lowest. This approach also contributes to our high accuracy rates relative to past efforts.

In our algorithm, the uncertainty in tree segmentations mainly derives from the spacing threshold. In sparse forests where the tree spacing is large, we can use a relatively large threshold to isolate trees. However, the appropriate threshold is difficult to determine in dense forests. A higher threshold can result in under-segmentations whereas a smaller threshold can result in over-segmentations. Over- and under-segmentations can be reduced by using an adaptive threshold, assuming that taller trees have larger crown diameters and hence larger spacing at the upper level. Alternatively, we can use a relatively small threshold to reduce under-segmentations, and incorporate more classification rules (e.g., the shape and distribution of the points) to reduce over-segmentations. We show that this adaptive threshold approach is sufficient in conifer forests in this study. In other forests, such as those dominated by deciduous trees with larger and more complex crowns and elongated branches, more object-oriented and shape-related rules should be incorporated to improve the accuracy. We plan to investigate this issue in future work. Meanwhile, it is worth noting that the algorithm is computation-intensive as the points are assigned to their corresponding tree clusters one by one. Adding more rules will signifi-cantly increase the computation time. Therefore, strategies (e.g., parallel processing) to reduce the computation time could be investigated.

Our algorithm is novel in that it works directly with the raw lidar point cloud. Most other individual tree algorithms make use of a gridded transformation of the point cloud: usually the canopy height model (Chen *et al.*, 2006). These methods are challenged in two ways. First, the uncertainty introduced by the interpolation method can affect the accura-cies of both the segmentations and tree measurements (Guo *et al.*, 2010). Second, these tree objects do not take advantage of the full 3D structure inherent in the lidar point cloud. With this new method, once the trees are correctly segmented, we can directly measure tree height, crown size, and other important tree parameters from the points contained in that tree. The advantage is obvious: tree segmentations and the consequent measurements are not affected by the uncertainty

of interpolation, and the important 3D forest parameters can be extracted directly from the lidar returns that make up each tree. In this study we focus on evaluating the accuracy of individual tree segmentations, and we plan to comprehensively evaluate the accuracy of tree measurements based on different tree segmentation methods in future research.

The accuracy assessment methods also need further investigation. In tree segmentation we aim to detect as many trees as possible while minimizing the number of falsely detected trees. There are two types of errors: commission error (*FP*) and omission error (*FN*), which result from over-segmentation and under-segmentation, respectively. In order to evaluate how well an algorithm performs, it is necessary to consider both types of errors in accuracy assessment. Remember that our interest focuses on one class, i.e., tree extraction (true positive), and true negative is not considered. Hence, traditional accuracy indices such as total accuracy and kappa coefficient are not applicable. Here we recommend the *F*-score, which is commonly used in information retrieval (Goutte and Gaussier, 2005; Sokolova *et al.*, 2006). *F*-score is the harmonic mean of precision and recall. Note that recall is inversely related to omission error, and precision is inversely related to commission error. Hence, a higher *F*-score indicates that both commission and omission errors are lower. In future research, it is necessary to comprehensively investigate the accuracy assessment methods in tree segmentations and propose a standard that can be applied consistently, which will facilitate accuracy comparison across the literature.

Conclusions

In this study we develop a new algorithm to segment individual trees from the lidar point cloud. The new algorithm adopts a top-to-bottom region growing approach that segments trees individually and sequentially from the tallest to the shortest. The algorithm performs well at segmenting trees from the lidar point cloud in complex mixed conifer forests on rugged terrain. The accuracies, in terms of recall, precision and *F*-score, are relatively high, indicating that the new algorithm has good potential for use in other forested areas.

Acknowledgments

References

Alexander, C., 2009. Delineating tree crowns from airborne laser scanning point cloud data using Delaunay triangulation, *International Journal of Remote Sensing*, 30(14):3843–3848.

Brandtberg, T., T.A. Warner, R.E. Landenberger, and J.B. McGraw, 2003. Detection and analysis of individual leaf-off tree crowns in small footprint, high sampling density lidar data from the eastern deciduous forest in North America, *Remote Sensing of Environment*, 85(3):290–303.

Chasmer, L., C. Hopkinson, P. Treitz, H. McCaughey, A. Barr, and A. Black, 2008. A lidar-based hierarchical approach for assessing MODIS fPAR, *Remote Sensing of Environment*, 112(12):4344–4357.

Chen, Q., D. Baldocchi, P. Gong, and T. Dawson, 2008. Modeling radiation and photosynthesis of a heterogeneous savanna woodland landscape with a hierarchy of model complexities, *Agricultural and Forest Meteorology*, 148(6-7):1005–1020.

Chen, Q., D. Baldocchi, P. Gong, and M. Kelly, 2006. Isolating individual trees in a savanna woodland using small footprint lidar data, *Photogrammetric Engineering & Remote Sensing*, 72(8):923–932.

Chen, Q., P. Gong, D. Baldocchi, and Y.Q. Tian, 2007. Estimating basal area and stem volume for individual trees from lidar data, *Photogrammetric Engineering & Remote Sensing*, 73(12): 1355–1365.

Dubayah, R.O., and J.B. Drake, 2000. Lidar remote sensing for forestry, *Journal of Forestry*, 98(6):44–46.

Falkowski, M.J., A.T. Hudak, N.L. Crookston, P.E. Gessler, E.H. Uebler, and A. Smith, 2010. Landscape-scale parameterization of a tree-level forest growth model: a k-nearest neighbor imputation approach incorporating LiDAR data, *Canadian Journal of Forest Research*, 40(2):184–199.

Falkowski, M.J., A.M.S. Smith, A.T. Hudak, P.E. Gessler, L.A. Vierling, and N.L. Crookston, 2006. Automated estimation of individual conifer tree height and crown diameter via two-dimensional spatial wavelet analysis of lidar data, *Canadian Journal of Remote Sensing*, 32(2):153–161.

Gaveau, D.L.A., and R.A. Hill, 2003. Quantifying canopy height underestimation by laser pulse penetration in small-footprint airborne laser scanning data, *Canadian Journal of Remote Sensing*, 29(5):650–657.

Glenn, N.F., D.R. Streutker, D.J. Chadwick, G.D. Thackray, and S.J. Dorsch, 2006. Analysis of LiDAR-derived topographic information for characterizing and differentiating landslide morphology and activity, *Geomorphology*, 73(1-2):131–148.

Goutte, C., and E. Gaussier, 2005. A probabilistic interpretation of precision, recall and F-score, with implication for evaluation, *Advances in Information Retrieval*, 3408:345–359.

Guo, Q., M. Kelly, P. Gong, and D. Liu, 2007. An object-based classification approach in mapping tree mortality using high spatial resolution imagery, *GIScience & Remote Sensing*, 44(1): 24–47.

Guo, Q., W. Li, H. Yu, and O. Alvarez, 2010. Effects of topographic variability and lidar sampling density on several DEM interpolation methods, *Photogrammetric Engineering & Remote Sensing*, 76(6):701–712.

Heurich, M., Å. Persson, J. Holmgren, and E. Kennel, 2004. Detecting and measuring individual trees with laser scanning in mixed mountain forest of central Europe using an algorithm developed for Swedish boreal forest conditions, *International Archives of Photogrammetry, Remote Sensing and Spatial Inforation Sciences*, XXXVI(8/W2):307–312.

Hopkinson, C., L. Chasmer, C. Young-Pow, and P. Treitz, 2004a. Assessing forest metrics with a ground-based scanning lidar, *Canadian Journal of Forest Research*, 34(3):573–583.

Hopkinson, C., M. Sitar, L. Chasmer, and P. Treitz, 2004b. Mapping snowpack depth beneath forest canopies using airborne lidar, *Photogrammetric Engineering & Remote Sensing*, 70(3):323–330.

Huang, S., S.A. Hager, K.Q. Halligan, I.S. Fairweather, A.K. Swanson, and R.L. Crabtree, 2009. A comparison of individual tree and forest plot height derived from lidar and InSAR, *Photogrammetric Engineering & Remote Sensing*, 75(2):159–167.

Koch, B., U. Heyder, and H. Weinacker, 2006. Detection of individual tree crowns in airborne lidar data, *Photogrammetric Engineering & Remote Sensing*, 72(4):357–363.

Korpela, I., B. Dahlin, H. Schäfer, E. Bruun, F. Haapaniemi, J. Honkasalo, S. Ilvesniemi, V. Kuutti, M. Linkosalmi, J. Mustonen, M. Salo, O. Suomi, and H. Virtanen, 2007. Single-tree forest inventory using lidar and aerial images for 3D treetop positioning, species recognition, height and crown width estimation, *IAPRS*, XXXVI:227–233.

Kwak, D., W. Lee, J. Lee, G.S. Biging, and P. Gong, 2007. Detection of individual trees and estimation of tree height using LiDAR data, *Journal of Forest Research*, 12(6):425–434.

Lang, S., D. Tiede, B. Maier, and T. Blaschke, 2006. 3D Forest structure analysis from optical and LIDAR data, *Revista Ambiência, Guarapuava, v.2 Edição Especial*, 1:95–110.

Lee, H., K.C. Slatton, B.E. Roth, and W.P. Cropper JR, 2010. Adaptive clustering of airborne LiDAR data to segment individual tree crowns in managed pine forests, *International Journal of Remote Sensing*, 31(1):117–139.

Lee, S.-J., Y.-C. Chan, D. Komatitsch, B.-S. Huang, and J. Tromp, 2009. Effects of realistic surface topography on seismic ground motion in the Yangminshan region of Taiwan based upon the spectral-element method and LiDAR DTM, *Bulletin of the Seismological Society of America*, 99(2A):681–693.

Lefsky, M.A., W.B. Cohen, G.G. Parker, and D.J. Harding, 2002. Lidar remote sensing for ecosystem studies, *BioScience*, 52(1):19–30.

Lim, K., P. Treitz, M. Wulder, B. St-Onge, and M. Flood, 2003. LiDAR remote sensing of forest structure, *Progress in Physical Geography*, 27(1):88–106.

Morsdorf, F., E. Meier, B. Allgöwer, and D. Nüesch, 2003. Clustering in airborne laser scanning raw data for segmentation of single trees, *International Archives of Photogrammetry, Remote Sensing and Spatial Inforation Sciences*, 34(3/W13):27–33.

Mutlu, M., S.C. Popescu, C. Stripling, and T. Spencer, 2008. Mapping surface fuel models using lidar and multispectral data fusion for fire behavior, *Remote Sensing of Environment*, 112(1): 274–285.

Naesset, E., and K.-O. Bjerknes, 2001. Estimating tree heights and number of stems in young forest stands using airborne laser scanner data, *Remote Sensing of Environment*, 78(3):328–340.

Patenaude, G., R.A. Hill, R. Milne, D.L.A. Gaveau, B.B.J. Briggs, and T.P. Dawson, 2004. Quantifying forest above ground carbon content using LiDAR remote sensing, *Remote Sensing of Environment*, 93(3):368–380.

Persson, A., J. Holmgren, and U. Söderman, 2002. Detecting and measuring individual trees using an airborne laser scanner, *Photogrammetric Engineering & Remote Sensing*, 68(9):925–932.

Popescu, S.C., 2007. Estimating biomass of individual pine trees using airborne lidar, *Biomass and Bioenergy*, 31(9):646–655.

Popescu, S.C., and R.H. Wynne, 2004. Seeing the trees in the forest: using lidar and multispectral data fusion with local filtering and variable window size for estimating tree height, *Photogrammetric Engineering & Remote Sensing*, 70(5):589–604.

Popescu, S.C., R.H. Wynne, and R.F. Nelson, 2002. Estimating plot-level tree heights with lidar: Local filtering with a canopy-height based variable window size, *Computers and Electronics in Agriculture*, 37(1–3):71–95.

Popescu, S.C., R.H. Wynne, and R.F. Nelson, 2003. Measuring individual tree crown diameter with lidar and assessing its influence on estimating forest volume and biomass, *Canadian Journal of Remote Sensing*, 29(5):564–577.

Riaño, D., E. Chuvieco, S. Condés, J. González-Matesanz, and S.L. Ustin, 2004. Generation of crown bulk density for *Pinus sylvestris L.* from lidar, *Remote Sensing of Environment*, 92(3):345–352.

Riaño, D., E. Meier, B. Allgöwer, E. Chuvieco, and S.L. Ustin, 2003. Modeling airborne laser scanning data for the spatial generation of critical forest parameters in fire behavior modeling, *Remote Sensing of Environment*, 86(2):177–186.

Sokolova, M., N. Japkowicz, and S. Szpakowicz, 2006. Beyond accuracy, F-score and ROC: A family of discriminant measures for performance evaluation, *AI 2006: Advances in Artificial Intelligence* (A. Sattar and B.-H. Kang, editors), Springer Berlin, Heidelberg, pp. 1015–1021.

St-onge, B.A., and N. Achaichia, 2001. Measuring forest canopy height using a combination of lidar and aerial photography data, *International Archives of Photogrammetry and Remote Sensing*, 34:131–137.

Stephens, P.R., P.J. Watt, D. Loubser, A. Haywood, and M.O. Kimberley, 2008. Estimation of carbon stocks in New Zealand planted forests using airborne scanning lidar, *International Archives of Photogrammetry and Remote Sensing*, XXXVI:389–394.

Suárez, J.C., C. Ontiveros, S. Smith, and S. Snape, 2005. Use of airborne LiDAR and aerial photography in the estimation of individual tree heights in forestry, *Computers & Geosciences*, 31(2):253–262.

Tiede, D., G. Hochleitner, and T. Blaschke, 2005. A full GIS-based workflow for tree identification and tree crown delineation using laser scanning, *CMRT*, 29-30 August, Vienna, Austria, pp. 9–14.

Vepakomma, U., B. St-Onge, and D. Kneeshaw, 2011. Response of a boreal forest to canopy gap openings: Assessing vertical and horizontal tree growth with multi-temporal lidar data, *Ecological Applications*, 21:99–121.

Wehr, A., and U. Lohr, 1999. Airborne laser scanning-an introduction and overview, *ISPRS Journal of Photogrammetry and Remote Sensing*, 54(2–3):68–82.

Wing, M.G., A. Eklund, and J. Sessions, 2010. Applying LiDAR technology for tree measurements in burned landscapes, *International Journal of Wildland Fire*, 19(1):104–114.

Wulder, M.A., C.W. Bater, N.C. Coops, T. Hilker, and J.C. White, 2008. The role of LiDAR in sustainable forest management, *Forestry Chronicle*, 84(6):807–826.

Wynne, R.H., 2006. Lidar remote sensing of forest resources at the scale of management, *Photogrammetric Engineering & Remote Sensing*, 72(12):1310–1314.

Yu, X., J. Hyyppä, M. Vastaranta, M. Holopainen, and R. Viitala, 2011. Predicting individual tree attributes from airborne laser point clouds based on the random forests technique, *ISPRS Journal of Photogrammetry and Remote Sensing*, 66(1):28–37.